Electronic Supplementary Material (ESI) for Journal of Materials Chemistry A.

Supporting Information

Precious-Metal-Free Co-Fe-O_x Coupled Nitrogen-enriched Porous Carbon Nanosheets Derived from Schiff-base Porous Polymers as Superior Electrocatalysts for Oxygen Evolution Reaction

Xiaoqing Lin,[a] Xinzhe Li,[a] Feng Li,[a] Yiyun Fang,[a] Min Tian,[a] Xingcai An,[b] Yan Fu,[c]

Jun Jin[a*] and Jiantai Ma[a*].

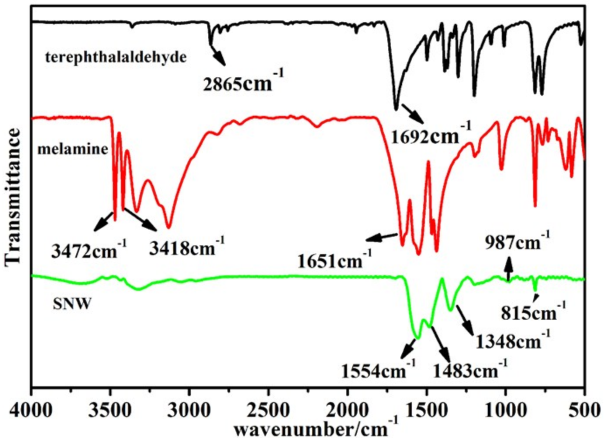

Figure S1.FTIR spectra of terephthalaldehyde , melamine and SNW

The signals of the triazine ring at 1554 cm^{-1}, 1483 cm^{-1}, and 1348 cm^{-1} are well resolved. Besides, the aromatic in-plane and out-of-plane deformation vibrations of the aldehyde components are detected at 987 cm^{-1}and 815 cm^{-1}[1].

.

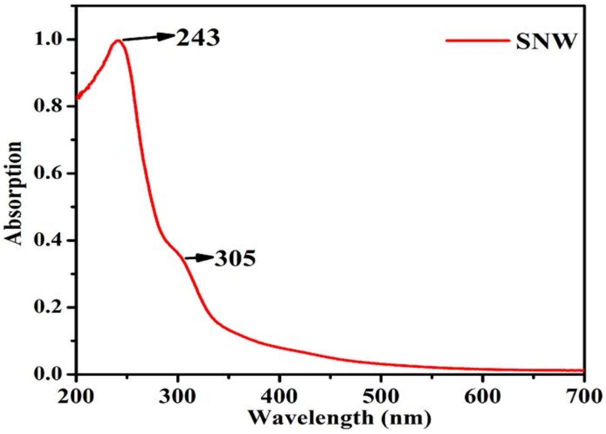

Figure S2 UV/Vis spectra of SNW

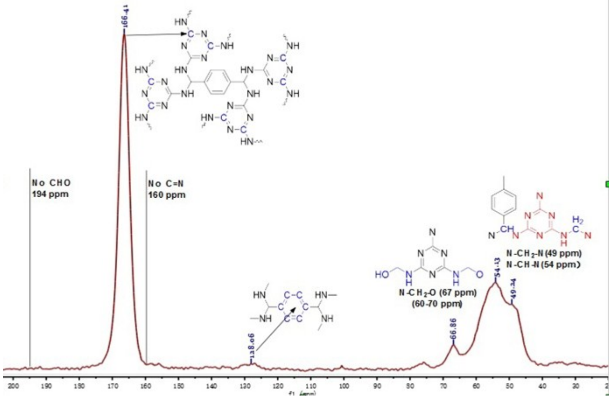

Figure S3. Cross-polarization (CP) ^{13}C MAS natural abundance NMR spectrum of SNW

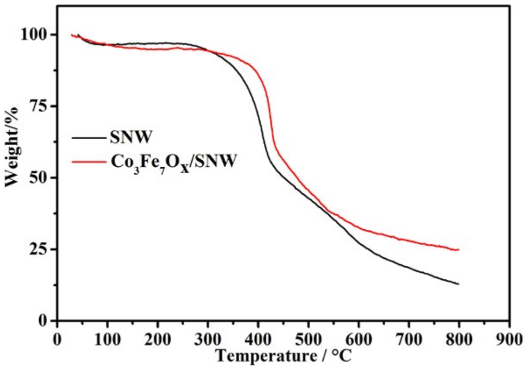

Figure S4. Thermogravimetric analysis of SNW and Co$_3$Fe$_7$O$_x$/SNW

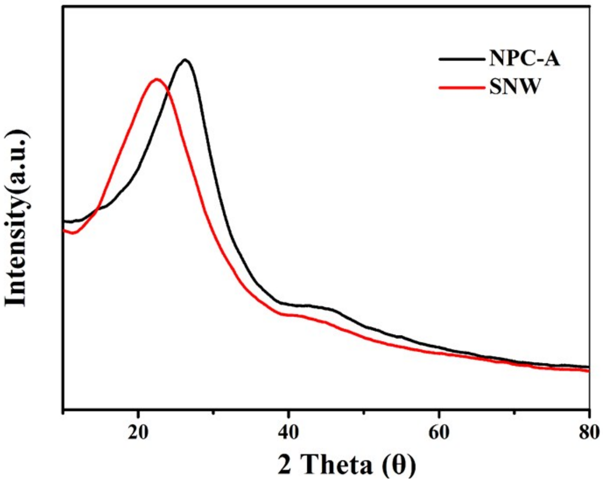

Figure S5 XRD patterns of SNW and SNW after pyrolysis at 450 ℃

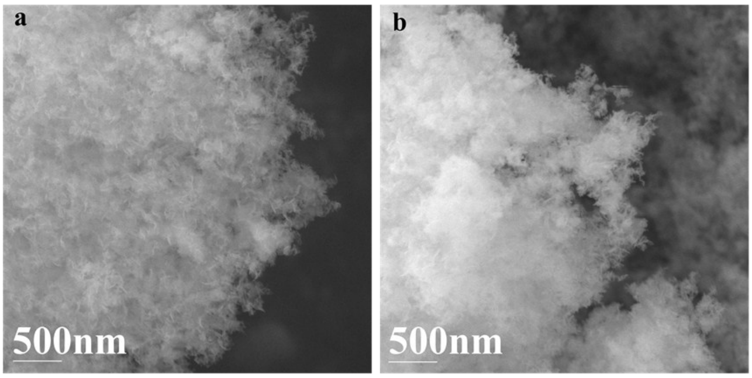

Figure S5 SEM images of $Co_3Fe_7O_x$/SNW

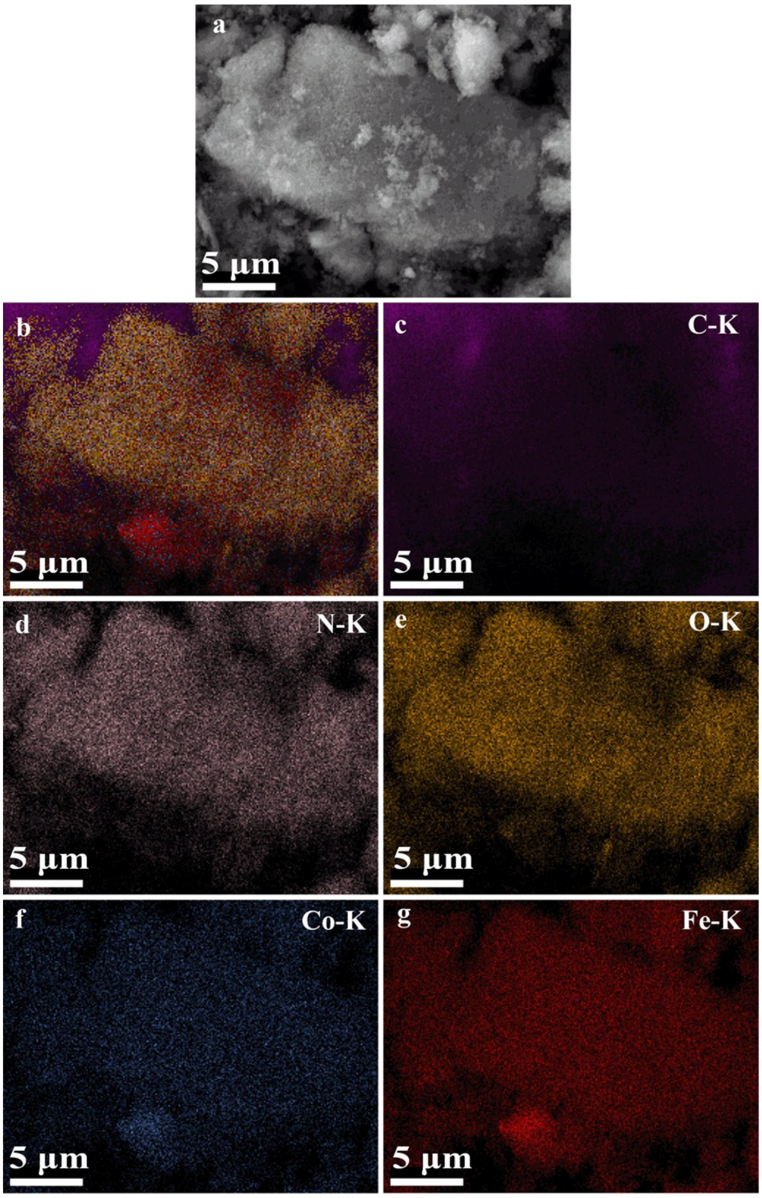

Figure S7 (a) SEM images of $Co_3Fe_7O_x$/NPC-450 (b) SEM elemental mapping showing distribution of C, N, O, Co and Fe atoms inside $Co_3Fe_7O_x$/NPC-450; (c-g) SEM elemental mapping showing distribution of C, N, O, Co and Fe atoms inside $Co_3Fe_7O_x$/NPC-450.

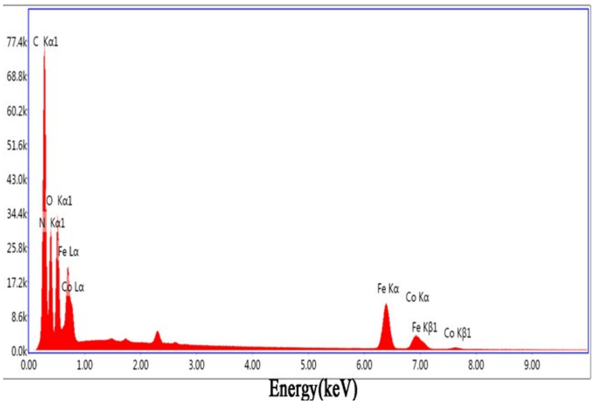

Figure S8. SEM-EDAX spectrum of $Co_3Fe_7O_x$/NPC-450

Table S1 Summary of actual percent of atom in $Co_3Fe_7O_x$/NPC-450 comes from SEM-EDAX spectrum

Element	**Weight%**	**Atom%**	**Intensity**
C K	29.70	40.05	3049.5
N K	30.24	34.96	1239.9
O K	18.64	18.86	1363.7
Fe K	15.51	4.50	1029.5
Co K	5.91	1.62	306.4

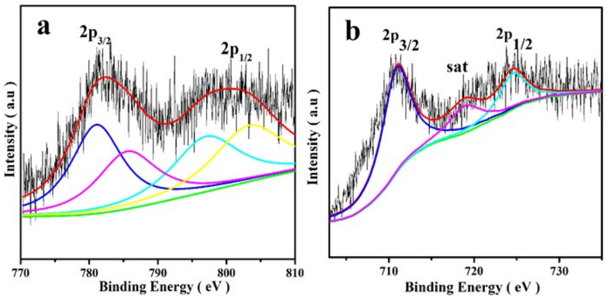

Figure S9. Co 2p (a) and Fe 2p (b) XPS spectra survey of $Co_3Fe_7O_x$

Co 2p (Fig. S9a) can be grouped into two pairs of peaks at 781, 797, 785.5 and 803.3 eV. The peaks centered at 781 and 797 eV are of Co $2p_{3/2}$and Co $2p_{1/2}$, respectively. The satellite peaks at around 785.5 (Co $2p_{3/2}$) and 803.3 eV (Co $2p_{1/2}$) are attributed to the two shake-up type peaks of Co at the high binding energy edge. The Fe 2p (Fig. S9b) spectra are deconvoluted into three peaks. The peaks at 710.9 eV and 724.8 eV are assigned to Fe $2p_{3/2}$ and Fe $2p_{1/2}$, respectively. The peak at 718.9 eV is a satellite peak [2, 3] .

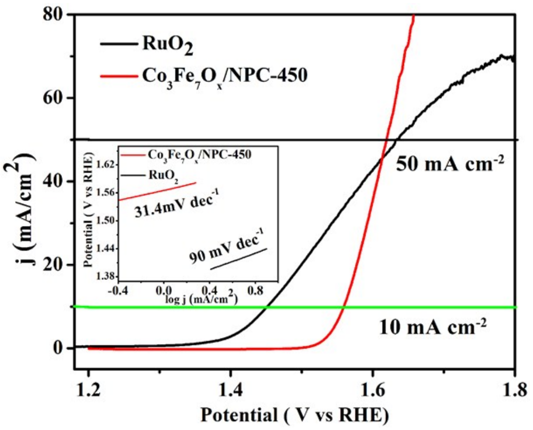

Figure S10. LSV scurves of $Co_3Fe_7O_x$/NPC-450 and RuO_2 in 1.0 M KOH solution, inset is Tafel plot of the catalysts above

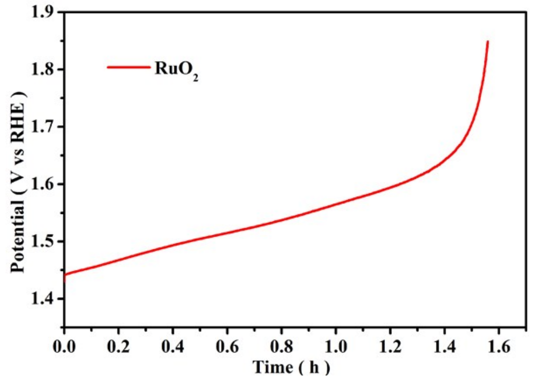

Figure S11 Chronopotentiometry curve of RuO_2 in 1.0 M KOH.

As shown in the LSVs curve (Fig. S10), the RuO_2 has high catalytic activity for OER with over-potential of 130mV to achieve a stable current density of 10 mA /cm^2. Unfortunately, it is not stable in alkaline solution (Fig. S11), which is in accordance with the report for the poor stability of RuO_2. Besides, the catalyst $Co_3Fe_7O_x$/NPC-450 approaches a large current density of 50 mA/cm^2 at an over-potential of 389 mV, which is low to that of RuO_2 reference (Fig. S10). As also observed, the Tafel slope value for the $Co_3Fe_7O_x$/NPC-450 (31.4 mV dec^{-1}) catalyst is much lower than that of RuO_2 (91.8 mV dec^{-1}), which confirms a faster increase of OER rate with the increasing potential (inset in Fig. S10).

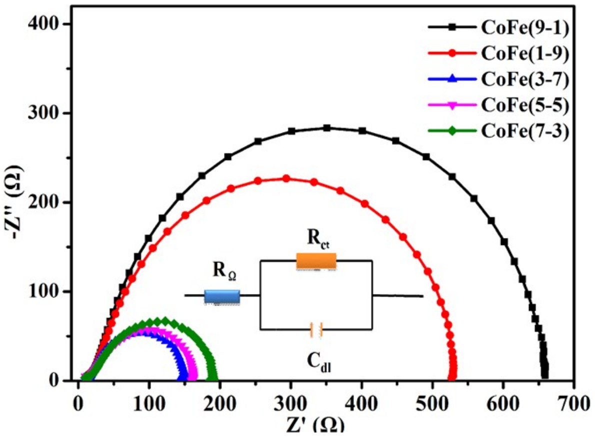

Figure S12. Co/Fe-ratio-dependent EIS plots under the bias of 1.54 V (vs. RHE).

Table S2 Summary of actual CoFe ratio and theirs catalysts for electrochemical OER

Target CoFe ratio	**Actual CoFe ratio**	**η@[10 mA cm^{-2}] [V]**	**Tafel slope [mV dec-1]**	**R$_Ω$ [Ω]**	**R$_{ct}$[a] [Ω]**
10:0	10:0	430	102	8.01	-
1:9	0.77:9.23	380	61.2	9.74	517
3:7	2.6:7.4	328	31.4	10.16	123.7
5:5	4.5:5.5	356	37.4	10.27	149.5
7:3	6.7:3.3	362	49.2	9.72	176.38
9:1	8.7:1.3	408	67.95	9.44	649
0:10	0:10	520	173	8.48	-

[a] Under the over-potential of 1.54 V (vs. RHE).

Table S3: Comparison of selected nonprecious OER electrocatalysts in alkaline media

Catalysts	**Electrolyte**	**η (mV) at 10mA/cm^2**	**Tafel slop （mV dec^{-1}）**	**Reference**
Co$_3$Fe$_7$O$_x$/NPC-450	1.0M KOH	328	31.4	This work

Co-P film	1.0M KOH	345	47	*Angew. Chem. Int. Ed.* 2015, 54, 6251.
NiCo LDH	1.0M KOH	367	40	*Nano Lett*. 2015, 15, 1421.
CoCo LDH	1.0M KOH	393	59	*Nat. Commun*. 2014, 5, 4477.
Co_3O_4/rm-GO	1.0M KOH	310	67	*Nat. Mater.* 2011, 10, 780.
CoO/NG	1.0M KOH	340	71	*Energy Environ. Sci.* 2014, 7, 609.
CoO_x film	1.0M KOH	403	42	*J. Am. Chem. Soc.* 2012, 134, 17253.
3D N-Doped Graphene/NiCo	0.1M KOH	>350	614	*Angew. Chem. Int. Ed.* 2013, 52, 13567.
CFO/rGO	1.0M KOH	340	31	*ChemSusChem*, 2015 8, 659
Co_3O_4/mMWCNT	0.1M KOH	390	65	*J. Mater. Chem. A*, 2013, 1, 12053
Co_3O_4/C	0.1M KOH	290	70	*J. Am. Chem. Soc*. 2014, 136, 13925.
Amorphous Ni-Co-O_x	1.0M KOH	330	39	*ACS Nano* 2014, 8, 9518.
Amorphous CoO_x	0.1M KOH	280	42	*Science* 2013, 340, 60
Amorphous $FeCoO_x$	1.0M KOH	290	33	*Science* 2013, 340, 60
Mesoporous Co_3O_4	1.0M KOH	480	/	*Nano Res*. 2013, 6, 47
Ni-Co_3O_4	1.0M KOH	370	65	*Int. J. Hydrogen Energy*, 2011, 36, 72
Nano-IrO_2	0.1M KOH	450	40	*J. Phys. Chem. Lett.* 2012, 3, 399.

[1] M.G. Schwab, D. Crespy, X. Feng, K. Landfester, K. Mullen, *Macromol. Rapid Commun*., 32 (2011) 1798-1803.

[2] J. Geng, L. Kuai, E. Kan, Q. Wang, B. Geng, *ChemSusChem*, 8 (2015) 659-664.

[3] S. Liu, W. Bian, Z. Yang, J. Tian, C. Jin, M. Shen, Z. Zhou, R. Yang, *J. Mater. Chem. A*, 2 (2014) 18012-18017.